HHS Public Access

Author manuscript

J Orthop Res. Author manuscript; available in PMC 2021 July 01.

Published in final edited form as:

J Orthop Res. 2020 July ; 38(7): 1607–1616. doi:10.1002/jor.24720.

Backside Wear of Tibial Polyethylene Components is Affected by Gait Pattern: A Knee Simulator Study using Rare Earth Tracer Technology

Valentina Ngai[1], **Joachim Kunze**[1,2], **Johannes Cip**[3], **Michel P. Laurent**[1], **Joshua J. Jacobs**[1], **Markus A. Wimmer**[1]

[1]Rush University Medical Center, Chicago, IL [2]Hamburg University of Technology, Germany
[3]Children Hospital St. Gallen, Switzerland

Abstract

The aim of this study was to determine the effect of two *in vivo*-determined gait patterns, one with low and one with high anteroposterior (AP) motion, on total and backside polyethylene insert wear in comparison with the ISO standard 14243–3. In order to differentiate and accurately quantify topside and backside wear, a novel technique was employed where different lanthanide tracers were incorporated into the polyethylene during manufacture. Wear particle analysis was conducted following established protocols. For all tested liners and motion protocols, the chemically calculated wear rates correlated closely with gravimetrically determined wear. Both *in vivo* motion groups displayed higher wear rates than the ISO group following the order of the AP motion amplitudes. Backside wear for ISO constituted 2.76% ± 0.90% (mean ± SE) of the total wear, increasing significantly to 15.8 ± 3.2% for the low AP and further increasing to 19.3 ± 0.95% for the high AP motion protocol. The mean wear particle sizes were under 200 nm for all three motion patterns, being largest for the protocol with high AP motion. Particle release from the low and high AP gait patterns was 1.9 to 2.8 times that from the ISO protocol. Testing for the proportion of backside wear across various activities of daily living should be an important consideration in evaluating knee prostheses wear.

Keywords

total knee prosthesis; backside wear; gait; polyethylene; rare earth

Correspondence: Markus A. Wimmer, PhD, Rush University Medical Center, 1611 W. Harrison Street, Suite 201, Chicago, IL 60612, Tel: (312) 942-2789, Fax: (312) 942-2101, markus_a_wimmer@rush.edu.

Author Contributions:

VN ran simulator experiments, analyzed wear rates and summarized results in a first draft; JK designed the tracer, provided the UHMWPE powder mixtures, and conducted ICP-MS measurements for wear analysis; JC performed the particle analysis and wrote this section of the manuscript; MPL conducted the statistical analysis, conceived the wear particle model and worked on the manuscript with MAW, JJJ provided clinical context and contributed to study design and tracer technology, MAW is responsible for the study design, conceived the tracer technology with JK, and wrote the final draft of the manuscript. All authors have read and approved the final submitted version of the manuscript.

Introduction

Wear of the ultra-high molecular weight polyethylene (UHMWPE) liner is a limiting factor in the longevity of total knee replacement (TKR)[1]. Wear particles may accumulate in tissues adjacent to the implant causing localized bone resorption (osteolysis) and subsequent implant loosening and failure. In particular, wear particles from the backside of the tibial liner have great osteolytic potential because of their small size[2]. In most knee designs, the backside of the liner is designed as a non-articulating surface; however, motion and forces on the articulating surface induce shear forces that challenge the locking mechanism and cause micromotion between the liner and metal tray[3]. Although generated motions are small, the large contact area between the insert backside and the tray can lead to substantial backside wear that is influenced by the input motion and forces at the articulation.

Pre-clinical wear evaluation on simulators is typically conducted using standardized protocols entailing either force (ISO 14243–1[4]) or displacement control (ISO 14243–3[5]). Ideally, the standard protocols replicate the *in vivo* motions and forces of TKR patients during walking in order to provide a realistic testing environment. Only a single force or motion waveform representing level walking is tested, although knee motions of TKR patients during level walking are variable and differ from the standardized input curves as shown recently[6]. In this study of 30 TKR patients, two distinct *in vivo* gait patterns emerged, one characterized as having low anteroposterior (AP-L) motion and the other high anteroposterior (AP-H) motion, although the AP motion amplitude for both groups was larger than specified in ISO standard 14243–3.

More closely replicating *in vivo* kinematics and kinetics in simulators would lead to more clinically relevant pre-clinical evaluation of polyethylene insert wear and implant performance. The primary aim of this study was therefore to determine the effect of these two *in vivo*-determined gait patterns[7] on total and backside insert wear in comparison with ISO standard 14243–3. We hypothesized that total wear and the relative contribution of backside wear to total wear would increase with increasing AP-motion because of the higher stresses applied to the polyethylene constraints and locking mechanism. A secondary aim was to compare the wear particle size and morphology and the estimated number of particles resulting from the in vivo-determined gait patterns and the ISO standard, given this can inform on polyethylene wear mechanisms[8] and potential biological effects[9]. We hypothesized that the number of particles produced would be dominated by the wear rate, so that the in vivo-determined gait patterns would lead to a greater particle load than the ISO standard pattern.

In order to differentiate and accurately quantify top and backside wear, we utilized a novel and validated technique where different lanthanide tracers are incorporated into the polyethylene during manufacture[10]. The amount of each tracer released into the lubricant during wear testing is proportional to the amount of polyethylene loss in the target areas.

Materials and Methods

Knee components for wear testing

Components from the Zimmer® NexGen® CR Knee Replacement System (Zimmer Biomet Holdings, Inc., Warsaw, Indiana, USA), a posterior cruciate-retaining (CR) fixed bearing knee system, were used in the wear tests. The cast cobalt-chrome femoral components (Cat. No. 5966-15-01; Size E, left) and titanium Ti-6Al-4V alloy tibial base plate (Cat. 5970-45-01, Size 5, pre-coat, no screw holes, pegged) were from stock, whereas the tibial inserts were specially manufactured using tracer-doped UHMWPE powder, as described below. The surface roughness Ra (arithmetic mean deviation), as determined on new components (n = 3) by white light scanning interferometry (NewView 6300 microscope, Zygo Corp., Middlefield, Connecticut, USA), was 73.0 ± 0.6 nm (± standard deviation) for the articular surface of the femoral components and 304.2 ± 3.3 nm for the top surface of the base plates articulating with the backside of the tibial inserts. These standard deviations reflect the component-to-component variation.

Preparation of tracer-doped UHMWPE powder

The tracer substances utilized this study were based on the rare earth metals, Europium (Eu) and Gadolinium (Gd), since they are detectable with high precision and accuracy in proteinaceous solutions using mass spectrometry techniques[10]. To homogeneously distribute Eu and/or Gd throughout the UHMWPE powder, Eu- and Gd-stearates were prepared separately from commercially available rare earth nitrates and sodium octadecanoate. The rare earth stearates formed precipitates in aqueous solutions that were digested, filtered and washed thoroughly before being admixed to GUR 1050 UHMWPE powder (Ticona, Florence (KY) USA). Before mixing, the rare earth stearates were dissolved in ligroin (petroleum ether) by boiling and mixed with nascent GUR 1050 UHMWPE powder using ultrasound. After mixing, the ligroin was distilled using a rotation evaporator, and the powder was dried in an oven at 100°C. UHMWPE powder mixtures containing (mean ± SD) 49.1±1.5 ppm Eu and 68.8±1.6 ppm Gd were obtained and shipped to Zimmer Inc. (Warsaw, IN, USA). Prior to manufacturing the tibial polyethylene components, we tested the impact of tracer-doping on polyethylene wear. Using a pin on-disk testing configuration, we found that doping did not adversely affect the wear performance of conventional UHMWPE[11].

Manufacturing of rare earth doped tibial polyethylene components

Five lanthanide-doped NexGen CR tibial inserts were specially prepared by Zimmer, Inc., in order to mimic the commercially available product. Each liner was moulded with 12.3 grams of Eu-stearate doped UHMWPE powder placed on the bottom of the liner mould, 10 grams of virgin GUR1050 resin placed in the middle and 10 grams of Gd-stearate doped GUR1050 powder placed on top. The minimum articulation thickness of all the liners was 10 mm. The pressure moulding procedure used was the same used for production pieces. The backside of each part was machined to interlock with a NexGen CR tibial plate. All liners were packaged in a nitrogen environment and gamma sterilized at 25 – 37 kGy.

Simulator input profiles

Simulator input was obtained from gait data from 30 TKR subjects (implanted with NexGen CR prostheses) where two range of motion groups were identified and categorized (Figure 1); a low AP motion group (AP-L) and high AP motion group (AP-H)[7]. In comparison to the ISO standard, the two distinct patterns of gait both had significantly higher AP translation during stance phase and had directional differences in swing phase. The associated *in vivo* flexion/extension (FE) and internal/external (IE) rotation profiles were inputted into the simulator as well. Figure 1a–c shows the *in vivo* gait derived waveforms and those defined by ISO 14243–3 (2004). Knee axial contact forces were calculated for each subject using a mathematical model of the knee[12]. Since the model calculates contact forces for stance only, the axial force values during swing phase were adopted from the ISO standard (Figure 1d).

Wear Test

The wear test was conducted using a four-station hydraulically actuated knee simulator (Endolab, Rosenheim, Germany), operated under displacement-control. A single actuator controlled the flexion-extension rotation of four stations that were mechanically coupled. Two horizontal actuators controlled the AP translation and the internal-external rotation of the tibial component for each station using linear variable differential transformers as displacement sensors. Each of the four stations had an individual actuator to apply axial loads underneath the chamber base holding the tibial tray. The tibial trays were placed within the chamber base to allocate 70% axial force through the medial compartment, as specified by ISO 14243–3 (2004). A clear plexiglass chamber fit over each chamber base to contain the testing lubricant.

Prior to testing, the doped polyethylene liners were presoaked in the same lubricant used for testing for 8 weeks to ensure full saturation. Weekly lubricant samples were taken to verify via ICP-MS that rare earth did not leach out of polyethylene. Four of the tibial liners were used during testing and one served as a passive soak to correct for fluid absorption. The testing liners were locked in the matching tibial metal trays. The metal trays themselves were fixed within the chamber base using a polyurethane casting resin (Ren 205–3, Rencast 205–3, Huntsman Advanced Materials Americas Inc., Los Angeles, CA, USA).

The femoral components were mounted to cylindrical shafts using the same casting resin as for the plates. The shafts locked into the flexion/extension frame of the simulator. The alignment of the center of rotation was undertaken as per ISO 14242–3 (2004). Each station was filled with 250 ml of new born calf serum diluted with a distilled water mixture containing EDTA, tris-hydroxy-methylamine and sodium chloride to achieve a 30g/l protein content buffered at pH 7.6. Sodium azide was also added at a concentration of 0.3% of the total solution to retard bacterial growth. The temperature of the lubricant was maintained at 37°C. Stations were covered with latex balloons to minimize evaporation and contamination. Stations were also weighed before and after each testing interval to allow replacement of water in case of evaporation. Every 0.5 million cycles (Mc), the test was halted and the tibial liners were cleaned and weighed according to ASTM 2025 and F732[13, 14] to obtain gravimetric wear. The experiment was then continued with fresh lubricant. The tibial inserts were weighed on an analytical balance with a readout to 0.01 mg (Mettler Toledo,

Columbus, Ohio, USA). The weight value for each component was the average of three weighings. Gravimetric wear was determined by calculating the difference in component weight between two interval measurement points and correcting for the weight increase of the passive soak control during that same test interval. The passive soak control gained approximately 1.05mg/ Mc over the duration of the entire experiment.

Each insert was sequentially subjected to the three motion profiles in the order ISO, AP-L, AP-H. Each motion profile was tested for 2 Mc at 1 Hz. Subsequent to this testing, the ISO profile was repeated for 0.5 Mc to verify that the same wear rate would be obtained as for the initial 2 Mc ISO run, precluding any significant interaction between the motion profiles sequentially tested on the same insert. The number of replicates was n = 4, except for the ISO profile, for which it was n = 3, due a defective liner. This liner exhibited an unusually high wear rate during the ISO test and lost structural integrity during the first 0.5 Mc of the AP-L test. A replacement liner was used to complete the AP-L motion test to 1.5 Mc, so the slope fit to obtain the steady-state wear rate included data from 0.5 Mc to 1.5 Mc rather than to 2 Mc.

Chemically-Determined Wear

Lubricant samples from each of the four testing stations and the passive soak station were taken after every 0.5 Mc interval. Thorough bubbling with nitrogen ensured a homogenous solution prior to sample draw. 2 ml of lubricant was obtained from each station, weighed and lyophilized. In the analytical chemistry laboratory, the dried sample containing polyethylene particles and tracer material was then transferred into a quartz vessel and mixed with 4 ml of HNO_3 and 6 ml of H_2O. Using a microwave for 20 min, any containing polyethylene particles were digested at temperatures of 250°C and pressures up to 75 bar to release Eu and Gd into the medium. The Eu and Gd concentrations for each sample were then determined using inductively coupled plasma mass spectrometry (ICP-MS), as previously described[10]. The limit of detection was better than 0.01 μg/l. Knowing the total lubricant volume in the chamber, lyophilized sample weight, dilution factors for chemical analysis, and rare earth concentrations in the polyethylene liners, the localized (Eu – backside; Gd – topside) weight loss of the liners were calculated to provide the chemically-determined wear.

Particle Isolation and Analysis

For each gait protocol, serum lubricant was collected after the 0.5 Mc and 2 Mc time points from Stations 2 and 3 to be processed for polyethylene wear particle isolation and analysis. The particles were recovered from the lubricant using an acid digestion method[15]. A 0.1 – 0.3 ml aliquot of the serum lubricant was digested in 5 ml of 10.5 M HCl for one hour at 50°C. It was then diluted with methanol (1:100) and filtered under vacuum through a 0.1 μm pore polycarbonate membrane (Nuclepore, Whatman GE Healthcare Life Sciences, Buckinghamshire, UK). The membranes were gold sputtered and examined under a scanning electron microscope (SEM) at a magnification of 20,000x. The resulting micrographs were analyzed with the ImageJ software (version 1.51j, National Institutes of Health, Bethesda, MA, USA) for particle area (A) and perimeter (P), from which the equivalent circle diameter (ECD) and equivalent shape ratio (ESR) of the particles were calculated using the following equations[16]:

$$ECD = 2\sqrt{A/\pi}$$

$$ESR = l/w$$

where l, the equivalent length, and w, the equivalent width of the particle are given by:

$$l = \frac{P}{2} + w\left(1 - \frac{\pi}{2}\right)$$

$$w = \frac{P - \sqrt{P^2 - 4\pi A}}{\pi}$$

Each particle was categorized as rounded (ESR < 2), elongated (ESR = 2 to 5), or fibrillar (ESR > 5). The particle data for Stations 2 and 3 were combined into one data set to yield at least 2000 particles for each combination of time point and gait protocol. The number of particles released per gait cycle for each combination was estimated from the volumetric wear rate and the observed particle ECD distribution (rather than the average ECD), assuming that particle height was 1/3 of ECD[15].

Statistics

Comparison of the wear and wear rate values for the three motion groups (ISO, n = 3; AP-L, n = 4; AP-H, n = 4) was performed using one-way analysis of variance (ANOVA), blocking with respect to the insert, given that each insert was used for the three motions protocols. Data transformation for variance stabilization was performed as needed, using the Box-Cox method (Design Expert 9, Stat-Ease, Inc., Minneapolis, Minnesota, USA). Post hoc pair-wise comparisons between motion groups (e.g., AP-L versus ISO) were performed using the ANOVA generated pooled standard deviation. Run-in versus steady-state wear rate comparisons were undertaken using two-tailed paired t-tests. The ECD size distributions were compared using 2-tailed t-tests after log-transforming the data to achieve normality. The shape distributions were compared using chi-square tests. For reference, the significance level was set at $p = 0.05$. Reported data are displayed as mean ± SE (standard error) unless noted otherwise.

Results

For all tested liners during the 3 tested motion profiles, the chemically determined wear correlated closely with the gravimetrically calculated wear after soak correction, with coefficient of determination (R^2) values ranging from 0.801 to 0.999 for ISO, from 0.995 to 0.998 for AP-L and 0.953 to 0.997 for AP-H (Figure 2). For all three input profiles, the average slopes (calculated from all 4 stations) of the regression lines were not significantly different from 1 ($p = 0.899$, $p = 0.541$ and $p = 0.150$, for ISO, AP-L, and AP-H respectively, independent t-test), indicating that the gravimetric and chemical methods were

interchangeable. Eu and Gd were not detected for the passive soak samples, proving that leaching of the tracers did not occur.

The gravimetric wear rates for each profile decreased from run-in (first 0.5 Mc) to steady-state (from 0.5 to 2 Mc) (Figure 3), the decrease being statistically significant only for the AP-H profile (Table 1). For run-in, the wear rates for both *in vivo* motion groups were higher than for ISO (Figure 3), but the difference was significant only for the AP-H profile (Table 2). Also, the AP-H profile yielded a significantly higher run-in wear rate than the AP-L profile (Figure 3, Table 2). For steady-state, the averages also suggested an increasing wear rate from ISO to AP-L to AP-H (Table 1); however, statistical significance was not achieved (Table 2), although only marginally so for ISO vs. AP-H ($p = 0.059$). Repeating the ISO profile at the end of the test sequence (ISO Loop) resulted in a similar wear rate (9.2 ± 2.7 mg/Mc) to the ISO wear rate in steady-state (10.02 ± 3.71 mg/Mc) at the beginning of the sequence, the difference between the two not being statistically different ($p = 0.908$). This agreement ruled out any significant interaction between the motion profiles sequentially tested on the same insert.

Backside wear for ISO constituted an average of 2.76% ± 0.90% (mean ± SE) of the total wear, dramatically increasing to 15.8 ± 3.2% for AP-L and further increasing to 19.3 ± 0.95% for AP-H (Figure 4). These increases were found to be statistically highly significant ($p < 0.001$). The increase in backside wear in going from AP-L to AP-H was marginally not statistically significant ($p = 0.076$). Total gravimetric and chemically determined wear and the percentage of backside wear for each component are given in Table 3.

The mean wear particle sizes (ECD) were under 200 nm for the three gait patterns and two time points (0.5 Mc, 2 Mc) (Table 4), with more than 99.5% of the particles being submicron in all cases. The corresponding size distributions were lognormal with a skew toward the larger particles. For a given gait protocol, the mean particle sizes at 2 Mc differed significantly from those at 0.5 Mc ($p < 0.001$), but with no specific trend (Table 4). Although the AP-H gait protocol produced larger particles than the AP-L protocol at both time points, the difference was statistically different only at the 2 Mc time point (Table 5). The estimated number of polyethylene wear particles released based on the wear rate and the particle size distribution ranged from 2.0 million/cycle (ISO at 0.5 Mc) to a maximum of 5.5 million/cycle (AP-L at 0.5 Mc) (Table 6). Particle release from the AP-L and AP-H protocols was 1.9 to 2.8 times that from the ISO protocol. (Table 6).

The mean equivalent shape ratio (ESR) was almost the same across the three gait protocols and time points, ranging from 3.42 to 3.45. Concomitantly, the proportions of rounded, elongated, and fibrillar particles were also similar across the three gait protocols, hovering around 23%, 63%, and 14%, respectively. The difference between the three protocols with respect to the proportions of particles of each shape was not statistically significant ($p = 0.276$, chi-square test).

Discussion

This is one of the first studies to investigate the effect of gait variability on wear of total knee replacements and compare them with the displacement-controlled ISO standard. As hypothesized, larger AP motion at the articulating surface, as observed *in vivo*, increased on average both the overall wear and the percentage of backside-to-total wear, although statistical significance for overall wear was only achieved for run-in.

A novel aspect of this study was the use of a chemical tracer technique to specifically quantify backside wear on polyethylene tibial inserts. Throughout the last couple of decades, accurate quantification of backside wear has proven difficult. Methods have included analyses of retrieved inserts and measuring decreases in depth of manufacturer markings[17–20] and linear scans using laser surface profilometry of the backside of retrievals and subtracting these measurements from data of new, unworn, size-matched components[21,22]. In addition, micro-CT methods have been employed[23,24]. All methods have indicated that wear of the backside tibial liner is a significant contributor to overall component wear, and may actually be on the same magnitude or greater than the wear experienced on the front articulating surfaces[18, 20–22]. For the particular implant design tested, backside wear determined in the current study was found to constitute less than 20% of the overall component wear, with backside wear rates of less than 20 mm^3/ Mc (using UHMWPE density of 0.934mg/mm^3). ISO determined backside wear was approximately 3 mm^3/Mc. Teeter et al.[24] conducted an ISO wear test with a cruciate-retaining design similar to this study and found that backside wear was approximately four to six times lower than articular wear. The TKR design chosen for the current study utilized a peripheral snap fit capturing mechanism with bevelled edges. Also no screw holes were present in the metallic tray. Though peripheral snap fit capture mechanisms were shown to produce the least amount of backside wear compared to other locking mechanisms[19,25], the absence of the screw holes and markings could account for the decreased wear. Significant evidence of wear was typically present around screw holes in previous studies[19,21,25,26] and depths of wear were measured based on the depth of the original manufacturer's stamp suggesting that presence of unsmooth surfaces may have caused increased wear. Barnett et al. (2001)[27] tested tibial bearing components that were also held in place via peripheral snap fit capturing mechanism and found that backside wear occurred only under high kinematics.

While gait pattern has been investigated and discussed as a factor in the wear of polyethylene[7,28, 29], to the best of our knowledge, it has not been implicated with backside wear of TKR. Factors investigated to contribute to backside wear have been documented as front articular surface geometry (affecting the stress distribution through the liner), surface roughness of the metallic tray, tibial liner thickness, implant in situ time and the locking mechanism design[19,25,30]. The surface roughness of the metal trays has been reported to influence the total amount of backside wear by 80–87%[30]. However, though polished trays result in up to five times less wear than rough blasted trays, an increase in submicron particles with higher osteolytic potential was observed[30]. The ability of the locking mechanism to reduce micromotion of the back bearing surface has also been an issue of debate. Different designs categorized as linear, peripheral or central capture mechanisms have been evaluated for their contribution to the severity of backside wear[25].

The wear debris particle size was similar across the three gait protocols and two time points (0.5 Mc, 2 Mc), with all mean ECDs within 7% of the grand average of the mean ECDs, 177 nm. However, the cubic dependence of particle volume on diameter implies that just a 10% drop in particle diameter leads to a 37% increase in the number of particles, so even small diameter differences can have a significant effect on particle count. Thus, the estimated particle released rate during run-in was higher for the AP-L protocol (5.5 million/cycle) than for the AP-H protocol (4.7 million/cycle) (Table 6), even though the AP-L wear rate was 37% lower (Table 1). In parallel with the wear rates, both in-vivo-determined gait protocols led to particle release rates that were higher than the ISO protocol by factors of 1.9 to 2.8, indicating that the ISO protocol may substantially underestimate the particle load. The mean ECDs of 167 nm to 189 nm reported here are about half of the value of 380 ± 90 (SD) nm reported for the same knee implant system and polyethylene type (conventional gamma irradiated GUR 1050 UHMWPE)[31]. This difference in particle size may stem from the different lubricants that were used, namely, newborn calf serum diluted to 30 g/l of protein in our study, versus undiluted bovine calf serum, which typically has a protein content of about 60–70 g/l and a different albumin/gamma globulin ratio. The mean particle sizes reported here are also much lower than the mean particle size of 1.67 ± 0.7 μm reported by Shanbhag et al. (2000) for debris extracted from periprosthetic tissue in 18 failed total knee replacements. The difference might be related to improvements in particle detection and/or differences in knee design. The TKRs covered a range of manufacturers and cruciate retaining and cruciate sacrificing designs, that predate the NexGen system, and therefore used UHMWPE that was processed differently (e.g., ram extruded, net shape molded, gamma sterilized in air, etc.), which may significantly affect wear and particle size. Ultimately, a study of wear debris in periprosthetic tissue for the same NexGen system as studied here will be necessary for a rigorous comparison with the simulator results.

The similar proportions of rounded, elongated, and fibrillar particles among the three gait protocols at the two time points suggest that differences in particle biological effects among the protocols will be mainly confined to the number of particles. Particle shape and roughness have been shown to influence the inflammatory response in a murine model[32, 33], as measured by cytokine production, with rough fibrillar particles eliciting the greatest response and smooth rounded particles eliciting the least response. Particle roughness was not evaluated in our study.

There are several limitations possibly affecting the generalizability of the results. First, only the NexGen cruciate-retaining design (NexGen CR) was examined to limit the number of confounding variables. These results cannot be simply extrapolated to TKR designs with varying amounts of constraint. Highly conforming articulations may result in differing material loss due to differing wear mechanisms[34]. Second, only two walking patterns, characterized by low (AP-L) and high (AP-H) antero-posterior motion, were tested. There are potentially several gait patterns within the TKR population which all may have different effects on TKR wear. Next to a larger anteroposterior motion, an increase in the internal-external (IE) rotation may accelerate wear. For example, Kawanabe et al.[35] showed that the addition of a ±5-degree tibial rotation on the knee simulator increased the TKR wear rate from 1.7 mg/Mc to 10.6 mg/Mc. Third, we worked with ISO 14243–3 (2004), which has been replaced with an updated standard in 2014. The updated version mirrored the IE

motion directions of the original standard, possibly impacting wear. Fourth, the medial-lateral contact force ratio was set as 0.7:0.3, as specified by the standard, and was kept constant throughout stance phase. Variations in varus-valgus rotation or adduction-abduction motion can cause changes in external knee moments, thus altering the medial-lateral contact force ratio and resulting contact forces[36]. Fourth, the sample size was low (n = 3, 4), thus reducing the statistical power. Low sample size is not unusual for knee wear simulator studies because the tests are lengthy (months), labor intensive, and expensive[37]. For n = 4, it is estimated that an effect size of 2.1 standard deviations can be detected with a power of 0.8 at a significance probability of 0.05 (2-tailed paired t-test, G*Power Version 3.1.9.2, Universität Düsseldorf, Germany). Given the standard deviation of approximately 5.6 mg/Mc observed in this study across motion protocols, this sensitivity corresponds to 12 mg/Mc in a paired comparison of wear rates. This sensitivity was sufficient to detect significant differences across protocols during run-in, but not during steady-state. A risk for Type II error is thus present in our study, suggesting that the visible trend of increasing steady-state average wear rates from ISO to AP-L to AP-H (Figure 3) may be real. Doubling the number of replicates to n = 8 would increase the sensitivity to 6.5 mg/Mc, a number still above the observed differences in the steady-state wear rates, except for ISO to AP-H.

Conclusions

Both *in vivo* motion groups displayed higher wear rates than the group tested per the displacement-controlled simulator ISO standard 14243–3:2004, with the wear rates ranking in the same order as the AP motion amplitudes. Of particular note was the effect on the proportion of backside wear. Components tested under the *in vivo* motion profiles experienced 16 to 20 % backside-to-total component wear, compared to approximately 3% under the ISO standard. These findings suggest that patients that walk with higher sagittal translation, may be incurring more implant wear. Knee wear simulation under the ISO 2004 standard underestimated the extent of wear and damage expected *in vivo*, supporting previous reports[37,38,39]. This study also provides further support that knee motion and load conditions are the main contributors to polyethylene articular wear and surface damage, as previously described[27,40,41,42].

The wear debris particle size was similar across the three gait protocols and two time point (0.5 Mc, 2 Mc), with all mean ECDs within 7% of the grand average of the mean ECDs, 177 nm. It was estimated that the in vivo motion protocols yielded twice the number of particles compared to the ISO protocol at steady-state, mainly as a result of higher wear rates. The distribution of rounded, elongated, and fibrillar particles was similar across the three protocols, hovering around 23%, 63%, and 14%, respectively, at steady-state.

A unique aspect of this study was the use of lanthanide tracers to quantify separately backside wear and articular wear. Using this validated tracer technique[10,11], it was demonstrated that the proportion of backside wear is sensitive to motion, which suggests that it may vary significantly across various activities of daily living, such as stair ascent and descent, chair sitting and rising, jogging, and bicycling, in addition to walking. A significant effect of activity on total tibial insert wear has already been demonstrated in simulator wear

tests[31]. Testing for the proportion of backside wear may therefore be an important consideration in evaluating knee prostheses for wear.

Acknowledgments

We thank Tobias Uth, Diego Orozco and Robin Pourzal for technical assistance with the wear simulation and particle analysis. This work was supported by grants of the National Institutes of Health (NIAMS R01AR059843, MAW), the TTRF Research Foundation, Japan (MAW), and the Rush Arthritis and Orthopedics Institute. Materials were provided by Zimmer Inc. (Warsaw, IN); we are particularly grateful for the manufacturing of rare earth doped polyethylene components.

The study was selected for the 2019 HAP Paul Award of the International Society for Technology in Arthroplasty (ISTA).

JK, JJJ, and MAW disclose US patent 8,889,167 (2014) as broadly relevant to the work. Outside the scope of this manuscript, JJJ and MAW disclose grants from Zimmer Biomet, CeramTec, Medtronic, and Nuvasive, as well as stock options (JJJ) with Hyalex and Implant Protection.

References

1. Gallo J, Goodman SB, Konttinen YT, Wimmer MA, Holinka M. 2013 Osteolysis around total knee arthroplasty: a review of pathogenetic mechanisms. 9(9): 8046–58
2. Surace MF, Berzins A, Urban RM, Jacobs JJ, Berger RA, Natarajan RN, Andriacchi TP, Galante JO. 2002 Coventry Award paper. Backsurface wear and deformation in polyethylene tibial inserts retrieved postmortem. (404): 14–23
3. Wasielewski RC, Galante JO, Leighty RM, Natarajan RN, Rosenberg AG. 1994 Wear patterns on retrieved polyethylene tibial inserts and their relationship to technical considerations during total knee arthroplasty. (299): 31–43
4. International Organization for Standardization: Implants for surgery – Wear of total knee-joint prostheses – Part 1: Loading and displacement parameters for wear-testing machines with load control and corresponding environmental conditions for test (ISO 14243–1). Geneva.
5. International Organization for Standardization:. Implants for surgery - Wear of total knee-joint prostheses – Part 2: Loading and displacement parameters for wear-testing machines with displacement control and corresponding environmental conditions for test (ISO 14243–3). Switzerland.
6. Ngai V, Wimmer MA. 2009 Kinematic evaluation of cruciate-retaining total knee replacement patients during level walking: a comparison with the displacement-controlled ISO standard. J Biomech. 42(14): 2363–2368. [PubMed: 19651410]
7. Ngai V, Wimmer MA. 2015 Variability of TKR knee kinematics and relationship with gait kinetics: implications for total knee wear. Biomed Res Int. 2015: 284513 [PubMed: 25866770]
8. Williams PA, Clarke IC. 2009 Understanding polyethylene wear mechanisms by modeling of debris size distributions. Wear. 267 (1–4): 646–652.
9. Fisher J, McEwen HM, Tipper JL, Galvin AL, Ingram J, Kamali A, Stone MH, Ingham E. 2004 Wear, debris, and biologic activity of cross-linked polyethylene in the knee: benefits and potential concerns. Clin Orthop Relat Res. 428: 114–9
10. Kunze J, Ngai V, Koelling S, Jacobs JJ, Wimmer MA. 2013 The use of europiumstearate to trace polyethylene wear debris in joint fluid after prosthetic joint replacement - A feasibility study. Trends Appl Spectrosc. 10: 43–48 [PubMed: 24920867]
11. Ngai V, Wimmer MA, Kunze J. 2009 Rare earth stearates for wear determination of UHMWPE bearings. Wear. 267(1–4): 679–682
12. Lundberg HJ, Ngai V, Wimmer MA. 2012 Comparison of ISO standard and TKR patient axial force profiles during the stance phase of gait. Proc Inst Mech Eng H. 226(3): 227–34 [PubMed: 22558837]
13. American Society for Testing and Materials: Standard practice for gravimetric measurement of polymeric components for wear assessment (ASTM 2025). Pennsylvania.

14. American Society for Testing and Materials: Standard test method for wear testing of polymeric materials used in total joint prostheses (ASTM F732). Pennsylvania.
15. Scott M, Morrison M, Mishra SR, Jani S. 2005 Particle analysis for the determination of UHMWPE wear. J Biomed Mater Res B Appl Biomater. 73(2): 325–337. [PubMed: 15685611]
16. Sprecher C, Schneider E, Wimmer MA. 2004 Generalized size and shape description of UHMWPE wear debris. In Crosslinked and Thermally Treated Ultra-High Molecular Weight Polyethylene for Joint Replacements, edited by Kurtz SM, Gsell RA, and Martell J. West Conshohocken, PA: ASTM International STP1445: 3–15.
17. Crowninshield RD, Wimmer MA, Jacobs JJ and Rosenberg AG. 2006 Clinical performance of contemporary tibial polyethylene components. J Arthroplasty. 21(5): 754–761. [PubMed: 16877165]
18. Furman BD, Schmieg JJ, Bhattacharyya S, and Li S. 1999 Assessment of backside polyethylene wear in three different metal backed total knee designs. TransORS 45: 149.
19. Jayabalan P, Furman BD, Cotrell JM and Wright TM. 2007 Backside wear in modern total knee designs. HSS Journal. 3: 30–34. [PubMed: 18751767]
20. Li S, Scuderi G, Furman BD, Bhattacharyya S, Schmieg JJ and Insall JN. 2002 Assessment of backside wear from the analysis of 55 retrieved tibial inserts. Clin Othop Rel Res. 404: 75–82.
21. Conditt MA, Thompson MT, Usrey MM, Ismaily SK and Noble PC. 2005 Backside wear of polyethylene tibial inserts: Mechanism and magnitude of material loss. J Bone J Surg Am. 87-A: 326–331.
22. Lavernia CJ, Sierra RJ, Hungerford DS and Krackow K. 2001 Activity level and wear in total knee arthroplasty: A study of autopsy retrieved specimens. J Arthroplasty. 16(4): 446–453. [PubMed: 11402406]
23. Sisko ZW, Teeter MG, Lanting BA, Howard JL, McCalden RW, Naudie DD, MacDonald SJ, Vasarhelyi EM. 2017 Current Total Knee Designs: Does Baseplate Roughness or Locking Mechanism Design Affect Polyethylene Backside Wear? Clin Orthop Relat Res. 475: 2970–2980. [PubMed: 28905208]
24. Teeter MG, Parikh A, Taylor M, Sprague J, Naudie DD. 2015 Wear and creep behavior of total knee implants undergoing wear testing. J Arthroplasty. 30(1): 130–4. [PubMed: 25175057]
25. Conditt MA, Stein JA and Noble PC. 2004 Factors affecting the severity of backside wear of modular tibial inserts. J Bone J Surg Am. 86-A: 305–311.
26. Engh GA, Dwyer KA and Hanes CK. 1992 Polyethylene wear of metal-backed tibial components in total and unicompartmental knee prostheses. J Bone J Surg Am. 74-B(1): 9–17.
27. Barnett PI, Fisher J, Auger DD, Stone MH and Eileen I. 2001 Comparison of wear in a total knee replacement under different kinematic conditions. J Mat Sci. 12: 1039–1042.
28. Davey SM, Orr JF, Buchanan FJ, Nixon JR, Bennett D. 2005 The effect of patient gait on the material properties of UHMWPE in hip replacements. Biomaterials. 26(24): 4993–5001. [PubMed: 15769535]
29. Tsao AK, Jones LC, Lewallen DG. 2008 What patient and surgical factors contribute to implant wear and osteolysis in total joint arthroplasty? J Am Acad Orthop Surg. 16 (Suppl 1): S7–13. [PubMed: 18612018]
30. Billi F, Aust S and Ebramzadeh E. 2007 Backside wear from polished tibial tray produces higher ratio of submicron particles. J Bone J Surg. 91-B(S1): 150.
31. Popoola OO, Yao JQ, Johnson TS, Blanchard CR. 2010 Wear, delamination, and fatigue resistance of melt-annealed highly crosslinked UHMWPE cruciate-retaining knee inserts under activities of daily living. J Orthop Res. 28(9): 1120–6. [PubMed: 20162713]
32. Yang SY, Ren W, Park Y, Sieving A, Hsu S, Nasser S, Wooley PH. 2002 Diverse cellular and apoptotic responses to variant shapes of UHMWPE particles in a murine model of inflammation. Biomaterials. 23(17): 3535–43. [PubMed: 12109677]
33. Sieving A, Wu B, Mayton L, Nasser S, Wooley PH. 2003 Morphological characteristics of total joint arthroplasty-derived ultra-high molecular weight polyethylene (UHMWPE) wear debris that provoke inflammation in a murine model of inflammation. J Biomed Mater Res A. 64(3): 457–64. [PubMed: 12579559]

34. Haider H, Weisenburger JN, Konigsberg BS, Hartman CW, and Garvin KL. 2018 For wear of total knee replacements, is higher or lower contact area better?, Award winning Poster in Adult Knee Reconstruction Category, P0199, Proceedings of the Annual Meeting of the American Academy of Orthopaedic Surgeons (AAOS), New Orleans, LA, March 2018.

35. Kawanabe K, Clarke IC, Tamura J, Akagi M, Good VD, Williams PA, Yamamoto K. 2001 Effects of A-P translation and rotation on the wear of UHMWPE in a total knee joint simulator. J Biomed Mater Res. 54(3): 400–6. [PubMed: 11189047]

36. Lundberg HJ, Foucher KC and Wimmer MA. 2009 A parametric approach to numerical modeling of TKR contact forces. JBiomech. 42: 541–545. [PubMed: 19155015]

37. Harman MK, DesJardins J, Benson L, Banks SA, LaBerge M and Hodge WA. 2009 Comparison of polyethylene tibial insert damage from in vivo function and in vitro wear simulation, J Orthop Res. 27: 540–548. [PubMed: 18932244]

38. Paul P 2004 Differences in polyethylene wear of revised, autopsy retrieved and simulator tested tibial knee implants. Master's thesis, University of Illinois at Chicago.

39. Schwenke T, Wimmer MA, Schneider E, Rosenberg A and Jacobs JJ. 2005 Kinetics and wear of retrieved and simulator tested implants in TKA, TransORS 51: 0835.

40. Blunn GW, Walker PS, Joshi A and Hardinge K. 1991 The dominance of cyclic sliding in producing wear in total knee replacements. ClinOrthop. 273: 253–260.

41. Harman MK, Banks SA, Hodge WA. 2001 Polyethylene damage and knee kinematics after total knee arthroplasty. Clin Orth Rel Res. 392: 383–393.

42. McEwen HMJ, Barnett PI, Bell CJ, Farrar R, Auger DD, Stone MG and Fisher J. 2005 The influence of design, materials and kinematics on the in vitro wear of total knee replacements. J Biomech. 38(2): 357–65. [PubMed: 15598464]

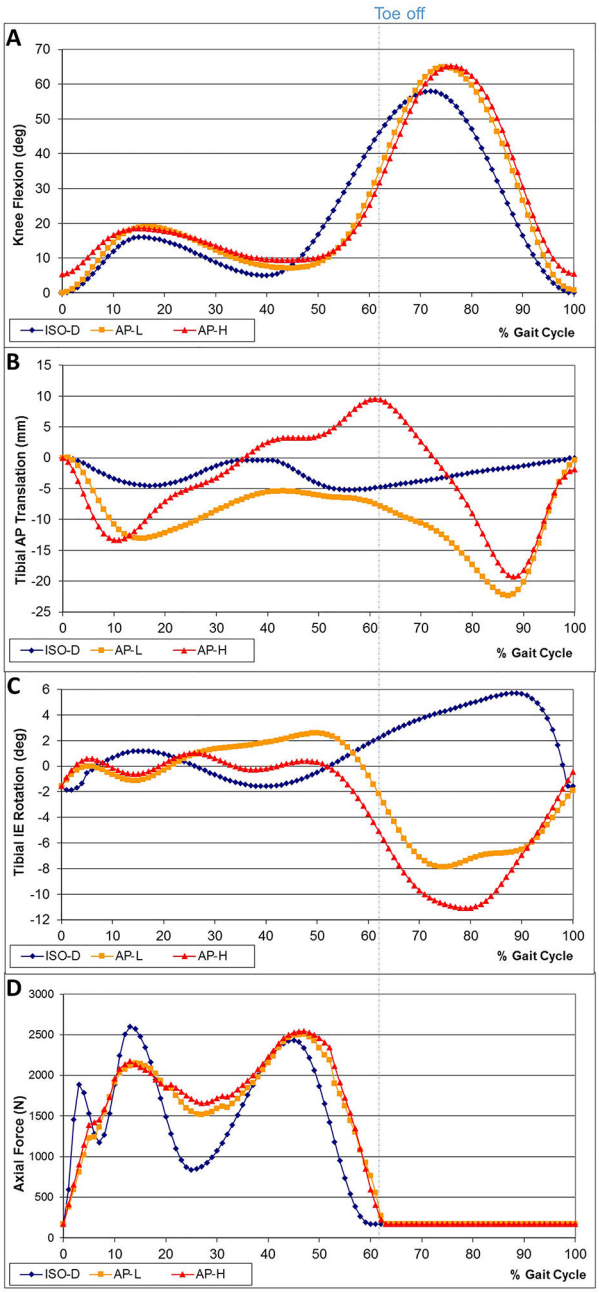

Figure 1:

Knee simulator input curves for ISO-D, AP-L and AP-H

a) FE rotation; b) AP translation; c) IE rotation; d) Axial force input

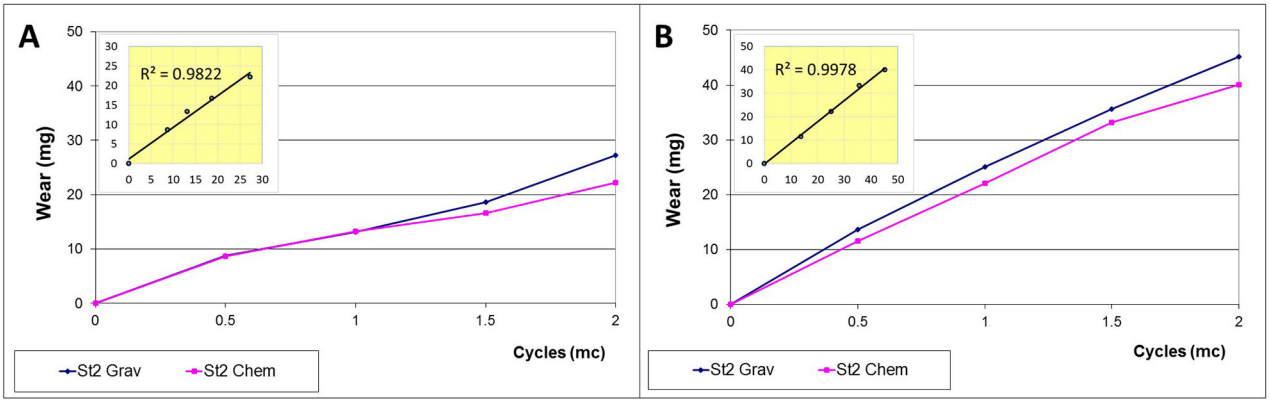

Figure 2:

Comparison of gravimetric (blue) and chemical (pink) wear over 2 million cycles (Mc) on Station 2 of the knee simulator. Measurements were taken in 0.5 Mc increments. The inlets demonstrate that both measurements were highly correlated.

a) ISO gait input; b) patient gait input (AP-L)

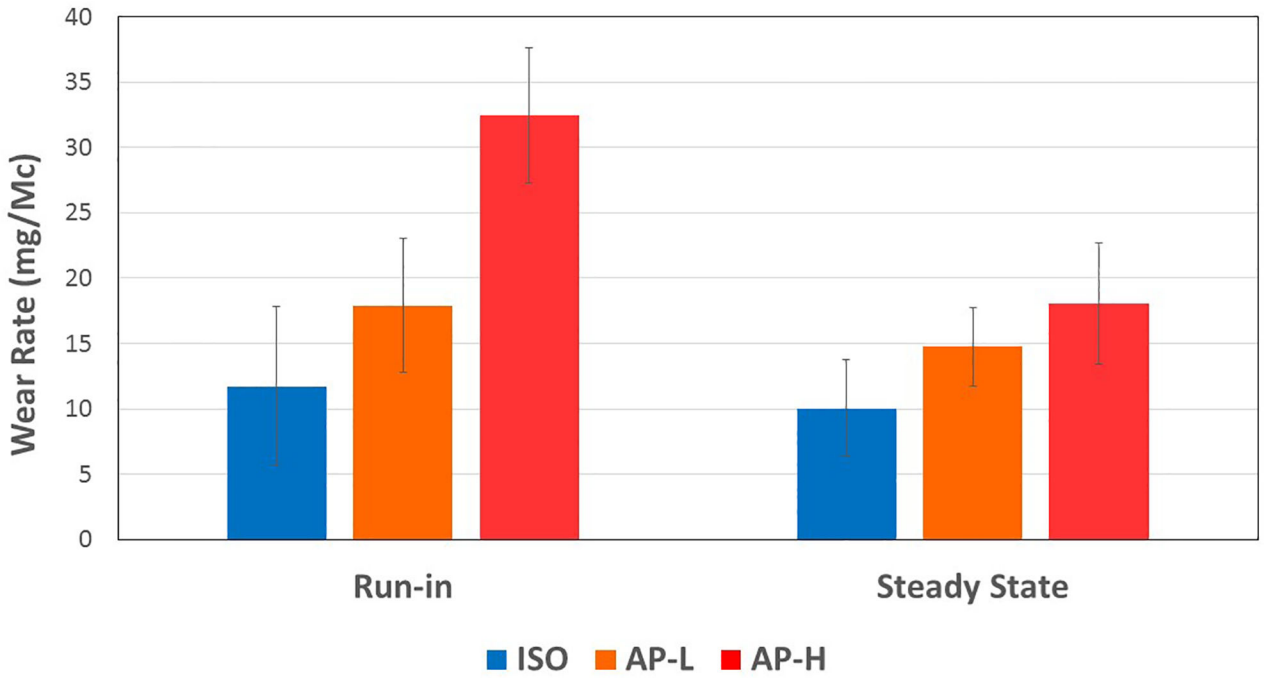

Figure 3:

Mean run-in and steady-state gravimetric wear rates of ISO-D, AP L and AP H.

The error bars correspond to ± SE. They do not reflect the scatter for statistical comparisons across wear regimes (run-in, steady-state) and across motion protocols because of the paired design of experiment where the same inserts were used across all motion protocols. For statistical comparisons, this paired or blocked experiment design reduces the error term markedly below what is suggested by the error bars in this graph.

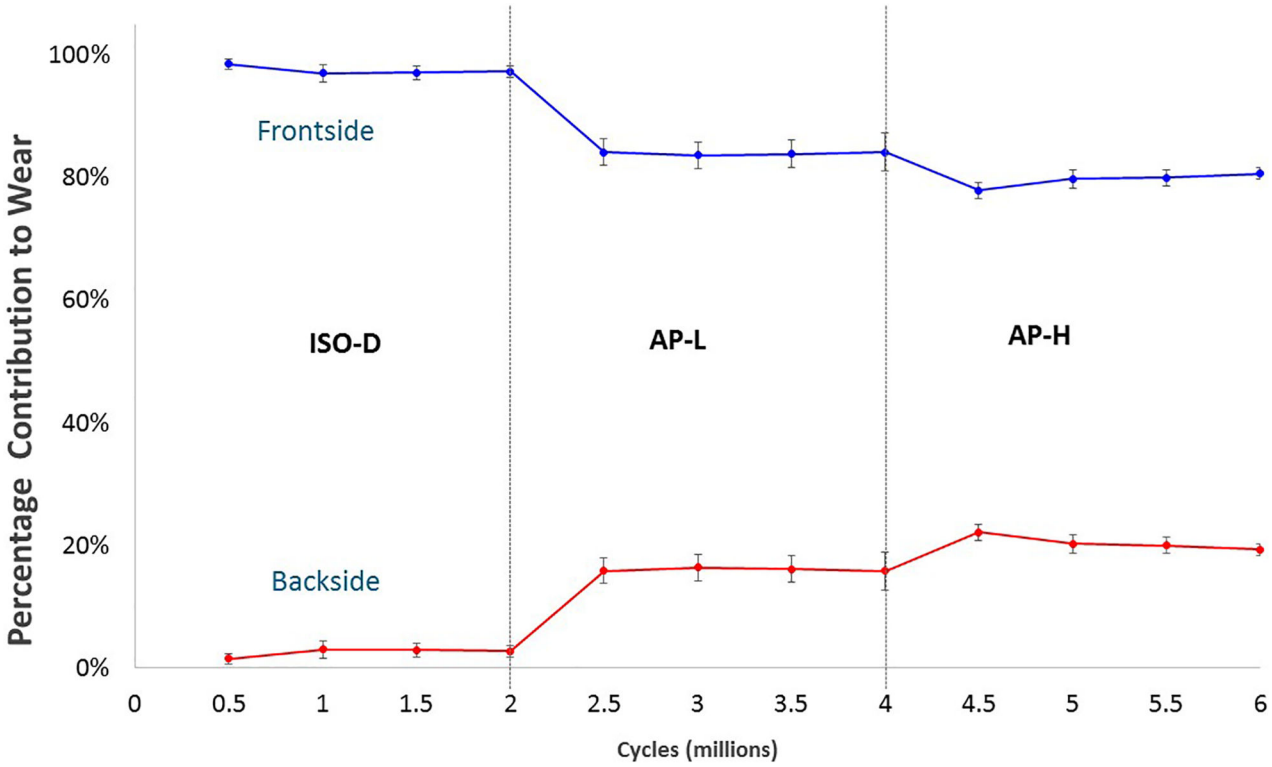

Figure 4:

Percentage contribution to the ongoing total chemically-determined wear by the topside and backside surfaces of the tibial inserts as a function of cumulative gait cycles. Each point is the mean for the particular gait protocol. For example, the point for backside wear at 3 Mc is the mean percentage backside wear after 1 Mc under AP-L gait. Error bars represent ± SE.

Table 1.

Run-in and steady-state gravimetric wear rates (mean ± SE) for the ISO-D, AP-L and AP-H gait protocols. The p values were obtained using a 2-tailed paired t-test comparing the run-in and steady-state wear rates.

Gait Protocol	Run-in Wear (mg/Mc)	Steady-state Wear (mg/Mc)	Ratio of Steady- state to Run-in	Significance P value
ISO	11.72 ± 6.09	10.02 ± 3.71	0.86	0.573
AP-L	20.43 ± 6.31	14.77 ± 3.02	0.82	0.457
AP-H	32.44 ± 5.17	18.06 ± 4.62	0.56	**0.025**

Table 2.

Statistical comparison of wear rates with respect to the motion profiles. Bold denotes statistical significance (ANOVA paired t-test, $p \leq 0.05$).

	Pairings	P value
Run-in	ISO vs. AP-L	0.154
	ISO vs. AP-H	**0.005**
	AP-L vs AP-H	**0.020**
Steady-state	ISO vs. AP-L	0.163
	ISO vs. AP-H	0.059
	AP-L vs AP-H	0.431

Table 3.

Total gravimetric and chemically-determined wear after 2 Mc and the corresponding contribution of backside wear to the total chemically-determined wear. Means ± SE.

	ISO	AP-L	AP-H
Total Gravimetric Wear (mg)	21.2 ± 8.5	31.6 ± 9.2	44.1 ± 9.2
Total Chemically-Determined Wear (mg)	19.5 ± 5.1	21.9 ± 9.1	37.3 ± 6.9
Percent Backside Wear	2.8% ± 0.9%	15.8% ± 3.2%	19.3% ± 0.9%

Table 4.

Wear particle size (ECD) statistics evaluated at the 0.5 Mc (run-in) and 2 Mc (steady-state) time points. All values are given in nm.

	0.5 Mc (Run-in)			2 Mc (Steady-state)		
	ISO	**AP-L**	**AP-H**	**ISO**	**AP-L**	**AP-H**
Mean	189.3	171.2	176.9	174.6	167.7	184.6
Std. Dev.	155.2	131.2	164.4	137.2	140.7	137.9
99% CI Low *	182.5	165.9	171.0	169.6	161.2	178.9
99% CI High *	196.4	176.6	183.0	179.7	174.4	190.6
p Value - 2 Mc vs. 0.5 Mc means **				<0.001	<0.001	<0.001

* Confidence interval for the mean, calculated on the log-transformed data and back transformed to the original scale.

** The p-values were calculated using 2-tailed t-tests on the log-transformed data. As a result, overlap in the 99% CIs may occur in the original scale, even though the p value is below 0.001.

Table 5.

Pairwise statistical comparison of the mean wear particle size (ECD) across motion profiles. The p-values were calculated using 2-tailed t-tests on the log-transformed data.

	Pairings	P value	Difference*
0.5 Mc	AP-L vs. ISO	<0.001	−9.6%
(Run-in)	AP-H vs. ISO	<0.001	−6.6%
	AP-L vs AP-H	0.344	−3.2%
2 Mc	AP-L vs. ISO	<0.001	−3.9%
(Steady-state)	AP-H vs. ISO	<0.001	5.8%
	AP-L vs AP-H	<0.001	−9.2%

*Difference = (AP-L - ISO)/ISO for AP-L vs. ISO, etc.

Table 6.

Estimated number of polyethylene particles released per cycle for the three gait protocols at the 0.5 Mc and 2 Mc time points.

	Particle Release Rate (MILLIONS per cycle)			Release Rate Relative to ISO	
Time Point	**ISO**	**AP-L**	**AP-H**	**AP-L**	**AP-H**
0.5 Mc (Run-in)	2.0	5.5	4.7	2.8	2.4
2 Mc (Steady-state)	2.2	4.0	4.6	1.9	2.1